ORGANOMETALLICS

Article

pubs.acs.org/Organometallics

Computational and Experimental Study on Selective sp^2/sp^3 or Vinylic/Aryl Carbon−Hydrogen Bond Activation by Platinum(II): Geometries and Relative Stability of Isomeric Cycloplatinated Compounds

Yumin Li,* Jeffrey Carroll, Bradley Simpkins, Deepak Ravindranathan, Christopher M. Boyd, and Shouquan Huo*

Department of Chemistry, East Carolina University, Greenville, North Carolina 27858, United States

Supporting Information

ABSTRACT: Cyclometalating ligands 6-(1-phenylethyl)-2,2′-bipyridine (**L4**), 6-(1-phenylvinyl)-2,2′-bipyridine (**L5**), and 6-(prop-1-en-2-yl)-2,2′-bipyridine (**L6**) were synthesized by the Negishi coupling of 6-bromo-2,2′-bipyridine with the corresponding organozinc reagents. The reaction of **L4** with K_2PtCl_4 produced only the cycloplatinated compound **4a** via sp^2 C−H bond activation. The reactions of **L5** and **L6** produced exclusively the cycloplatinated compounds **5b** and **6a**, respectively, via vinylic C−H bond activation. DFT calculations were performed on 12 possible cycloplatination products from the reaction of *N*-alkyl-*N*-phenyl-2,2′-bipyridin-6-amine (alkyl = methyl (**L1**), ethyl (**L2**), and isopropyl (**L3**)) and **L4**−**L6**. The results show that compounds **1b**−**3b** resulting from the sp^3 C−H bond activation of **L1**−**L3** are thermodynamic products, and their relative stability is attributed to the planar geometry that allows for a better conjugation. Similar reasoning also applies to the stability of products from vinylic C−H bond activation of **L5** and **L6**. The relative stability of isomeric cycloplatinated compounds **4a** and **4b** may be due to the different strengths of C−Pt bonds. The steric interaction is the major cause of severe distortion from a planar coordination geometry in the cycloplatinated compounds, which leads to instability of the corresponding cyclometalated products and a higher kinetic barrier for C−H bond activation.

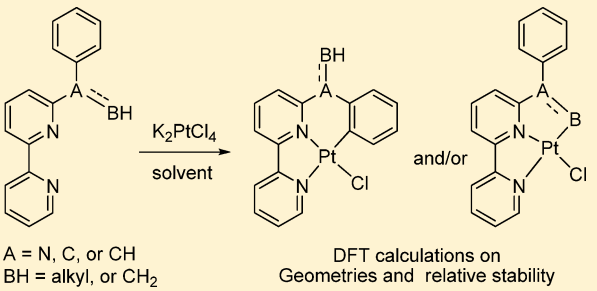

INTRODUCTION

Selectivity is a fundamental issue in chemical reactions. It is common that an organic or organometallic reaction can produce multiple products through different pathways. The product distribution is determined by the thermodynamic and kinetic factors of the reaction that are often influenced by reaction conditions, and selective formation of the desired product could thus be achieved by either thermodynamic control or kinetic control. In a reaction in which two or more isomeric compounds could be formed through similar and competitive mechanisms, a selective formation of one isomer is usually challenging but the most desirable in terms of efficiency in synthesis and product isolation and purification. In the recently reported cycloplatination of *N*-alkyl-*N*-phenyl-2,2′-bipyridin-6-amine (alkyl = methyl (**L1**), ethyl (**L2**), and isopropyl (**L3**)), the selective formation of the product from either the sp^2 C−H or the sp^3 C−H activation is controlled by the solvent used in the reaction (Scheme 1).[1] Selective sp^2/sp^3 C−H bond activation has been reported in other cycloplatination reactions,[2] and more examples can be found in the related cyclopalladation reactions;[3] however, cases with such a degree of control in which either isomer can be prepared with excellent selectivity are rare.[1,3a] Experimental results suggest that the product **1b** resulting from the sp^3 C−H bond activation of *N*-methyl-*N*-phenyl-2,2′-bipyridin-6-amine (**L1**) in acetic acid may be more stable, and the reaction is thermodynamically controlled.[1] One difference between **1a** and **1b** is that **1a** has a fused five−six-membered metallacyle, while **1b** has a fused five−five-membered ring. Although it has been suggested that a five-membered metal chelation is more

Scheme 1. C−H Bond Activation of 6-(*N*-Alkyl-*N*-phenylamino)-2,2′-bipyridine by K_2PtCl_4

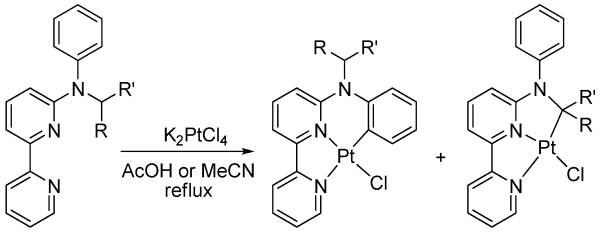

Received: April 17, 2015

DOI: 10.1021/acs.organomet.5b00326
Organometallics XXXX, XXX, XXX−XXX

stable than a six-membered chelation,[4] and in fact, six-membered cyclometalated platinum or palladium complexes are less common, other factors could also contribute to the relative stability of isomeric sp^2 and sp^3 C−H bond activation products **a** and **b**.

To further understand the selective C−H bond activation, it is necessary to carry out a systematic study on a series of closely related reactions. Especially, a combination of complementary experimental and theoretical studies would allow elucidation of details of the structure and relative stability of the products that could be formed in these reactions. Computational chemistry has played an increasingly important role in studying the mechanisms of organometallic C−H bond reactions.[5] In particular, density functional theory (DFT) has been frequently used to investigate the reaction mechanisms of real organometallic transformations including cycloplatination reactions,[6] since it allows for accurate calculations of a relatively large metal complex. Therefore, we decided to use DFT calculations to examine the relative stability of 12 isomeric cycloplatinated complexes that could be formed from cycloplatination of **L1**−**L3** and structurally related ligands **L4**−**L6** (Chart 1) and compare the results with those obtained experimentally to elucidate the thermodynamic control of the reaction. The cycloplatination of **L4** has been previously reported,[7] but we will reexamine it under different conditions. Ligands **L5** and **L6** are newly designed to examine the effect of structural variations on the control of selectivity in the cycloplatination reactions.

Chart 1

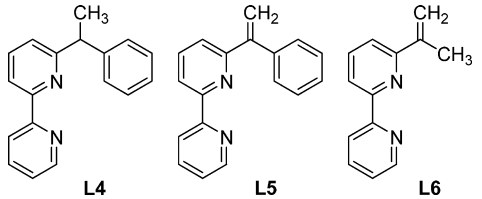

L4 L5 L6

RESULTS AND DISCUSSION

Cycloplatination of Ligands L4−L6. Ligand **L4** is structurally related to **L1**, with the only difference in the linking atom between the bipyridyl and the phenyl groups. It would be interesting to see if the solvent-controlled selective C−H bond activation of **L1** is also applicable to **L4**. The ligand **L4** was synthesized previously by a very sophisticated synthesis involving oxidation of 2-(1-phenylethyl)pyridine to the corresponding *N*-oxide, sequential treatments of the *N*-oxide with dimethyl sulfate and potassium cyanide to give 6-(1-phenylethyl)picolinonitrile, and the cocyclotrimerization of the nitrile with acetylene in the presence of (η^5-cyclopentadienyl)-cobalt-1,5-cyclooctadiene.[8] We report here a much simpler and straightforward synthesis of **L4**. By using Negishi coupling of (1-phenylethyl)zinc bromide,[9] which was generated in situ from direct insertion of zinc to (1-bromoethyl)benzene,[10] with 6-bromo-2,2′-bipyridine, ligand **L4** was synthesized in good yield (Scheme 2). It was found that the reaction of **L4** with K_2PtCl_4 in either acetic acid or acetonitrile produced **4a** through sp^2 C−H bond activation. The ^{1}H NMR spectrum of **4a** is consistent with that reported previously for the same compound prepared under different conditions,[7,11] showing the metalation at the phenyl ring. Complete assignment of the signal was accomplished by the 2D COSY experiments. Notably, H-6′ appears at 9.70 ppm and H-6″ appears at 8.10 ppm with the Pt−H-6″ coupling constant being 47 Hz. The reaction in acetonitrile is very sluggish, and no formation of **4b** was detected. These results indicate that **4a** could be both the kinetic and thermodynamic product, which is quite different from the reaction of **L1**, where the fused five−five-membered **1b** is thought to be the thermodynamic product.[1] It should be noted that the sp^3 C−H bond activation of 6-alkyl-2,2′-bipyridine by platinum was reported to preferentially form a fused five−five-membered platinacycle.[12]

The design of ligands **L5** and **L6** serves to further understand the structural effect on the selectivity of C−H bond activation. In **L5**, both vinylic and aryl C−H bonds are expected to have similar intrinsic reactivity, but the steric effect and the size of fused metallacycles may play a role in determining the product distribution in the cycloplatination reaction. In **L6**, the methyl (or allylic) C−H bonds and the vinylic C−H bonds may have different reactivity, but the products would have the same size of fused five−five-membered metallacycles. Both ligands **L5** and **L6** were prepared in high yields via Negishi coupling[13] in the presence of the catalyst $Pd(PPh_3)_4$, as shown in Scheme 3. Interestingly, reactions of **L5** and **L6** with K_2PtCl_4 produced cycloplatinated compounds **5b** and **6a**, respectively, as the sole product resulting from the vinylic C−H bond activation, regardless of the solvent used in the reaction: acetic acid or acetonitrile. Compounds **5a** and **6a** were characterized by elemental analysis, mass spectrometry, and ^{1}H NMR spectroscopy. The ^{13}C NMR spectra were not recorded because of poor solubility of the complexes. The ^{1}H NMR spectra of **5b** and **6a** show that the metalation occurs at the vinylic carbon, and the remaining vinylic hydrogen in **5a** and **6a** shifts to lower field upon metalation with a large Pt−H coupling constant, appearing at 7.95 ($^2J_{Pt-H}$ = 57 Hz) and 7.54 ppm ($^2J_{Pt-H}$ = 61 Hz), respectively. The chemical shifts of 6′ hydrogens in **5a** and **6b** are 8.97 and 8.96 ppm, respectively, which is

Scheme 2. Preparation of L4 and Its Cycloplatination Reaction

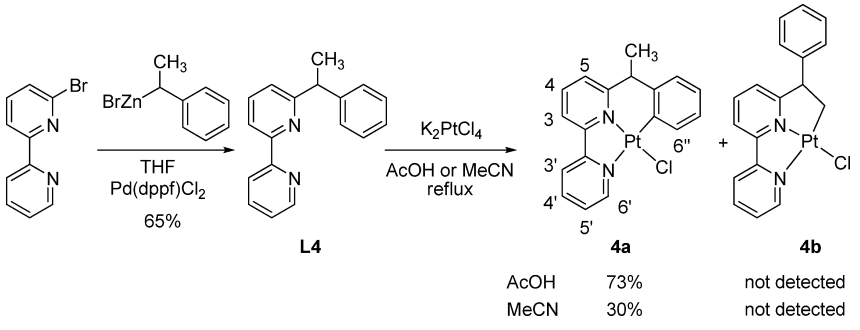

DOI: 10.1021/acs.organomet.5b00326
Organometallics XXXX, XXX, XXX−XXX

Scheme 3. Synthesis of Ligands L5 and L6 and Their Cycloplatination Reactions

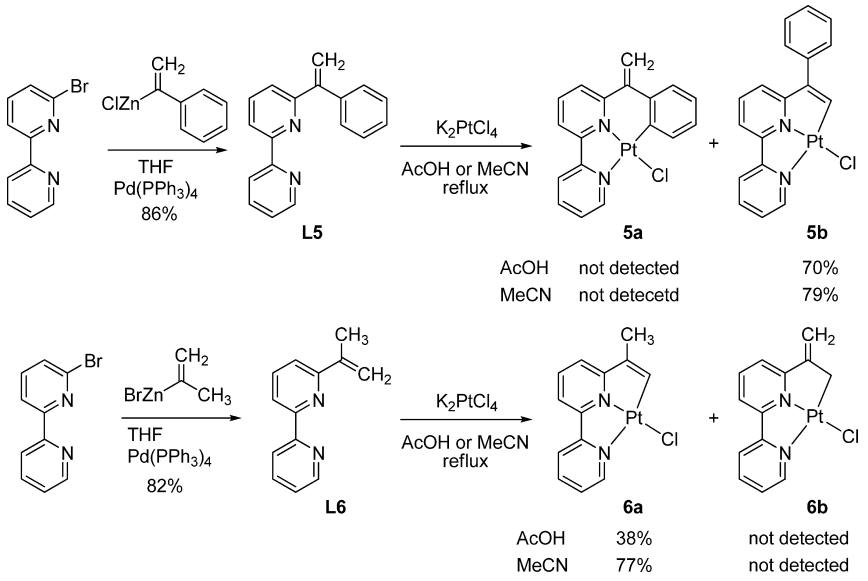

significantly smaller than that of H-6′ (9.70 ppm) in **4a**. Such a difference in deshielding effect on the H-6′ due to different sizes of fused platinacycles has been noted before.[12] The low yield of the reaction of **L6** in acetic acid is mainly attributed to the decomposition of platinum complexes since some black precipitates were formed during the reaction. The decomposition was not observed in the reaction in acetonitrile. When the reactions of **L5** and **L6** were run in AcOD, no deuterium scrambling was detected at the phenyl group and the methyl group in the products **5b** and **6a**. These results suggest that formation of **5b** and **6a** might be both kinetically and thermodynamically controlled.

The exclusive formation of **5b** and **6a** can be rationalized by considering the steric interaction between one of the vinylic H's and the 5-H of the pyridine ring in **L5** and **L6** (Chart 2), which

Chart 2

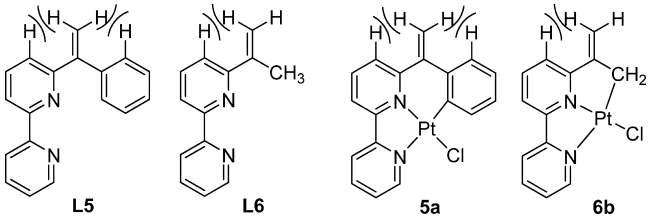

occurs when **L5** and **L6** have to adopt a proper conformation for the aryl C−H bond activation of **L5** and methyl (allylic) C−H bond activation of **L6**. Additional steric interaction exists between the other vinylic H and one of the *ortho* H's of the phenyl ring in **L5**. It can be expected that the stability of **5a** and **6b** would also suffer from such steric hindrance.

In general, for competing sp^2/sp^3 or vinylic/aryl C−H bond activations of compound **A** producing cycloplatinated compounds **B** and **C**, there are three possible scenarios, I, II, and III, as shown in Chart 3. If both reactions are irreversible, the product formation will be under kinetic control (I). On the other hand, if both reactions are reversible, the product formation will be thermodynamically controlled (II), and the ratio of the products is a reflection of their relative thermodynamic stability. If one reaction is reversible, while

Chart 3

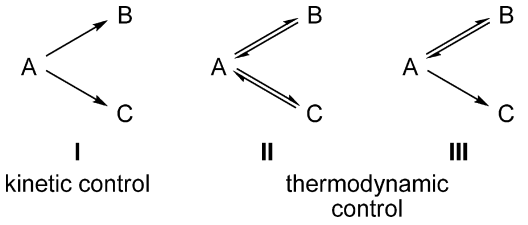

the other is irreversible (III), the thermodynamic product **C** would be the sole product, and the difference in their stability may have to be determined with a different method if the equilibrium could not be established between **B** and **C**.

The cycloplatination of **L1** in acetic acid very much resembles scenario III. Although **1b** was suggested to be the thermodynamic product in the reaction of **L1**, the formation of **1b** seemed to be irreversible, as suggested by a previous deuterium-labeling experiment, because the refluxing of **1b** in AcOD resulted in D scrambling only at the methylene carbon, but not at the *ortho* positions of the phenyl ring.[1a] On the other hand, the isomerization of **1a** or the cycloplatination of **L1** in AcOD resulted in about 90% D incorporation at both the methylene and the *ortho* positions of the benzene ring. Even with addition of concentrated DCl−D_2O, the reflux of **1b** in AcOD for 12 h did not lead to D incorporation to the *ortho* positions of the *N*-phenyl ring (Scheme 4). These D/H exchange experiments also suggest that in the reaction of **L1** with K_2PtCl_4 in acetic acid the likely reaction pathways involve the initial coordination of **L1** to the platinum salt to generate **7** and **8**, cyclometalation of **7** and **8** to produce **1a** and **9**, respectively, and a retro "rollover" cyclometalation[14] from **9** to **1a** and isomerization of **1a** to **1b**. A "rollover" cyclometalation from **7** to **9** may not be a favorable pathway under the conditions, as the isomerization of **1a** to **1b** in AcOD, which proceeds likely through deuterolysis of **1a** to give **7**-*d* (deuterated at the metalated carbon of the phenyl group) as the intermediate, did not lead to a measurable D/H exchange at the 3-position of the bipyridine ring. If the equilibrium between the two isomers **1a** and **1b** could not be established with an experiment, theoretical calculations would be the alternative

DOI: 10.1021/acs.organomet.5b00326
Organometallics XXXX, XXX, XXX−XXX

Scheme 4. D/H Exchange and "Rollover" Cyclometalation in the Reaction of L1 with K_2PtCl_4 in AcOH(D)

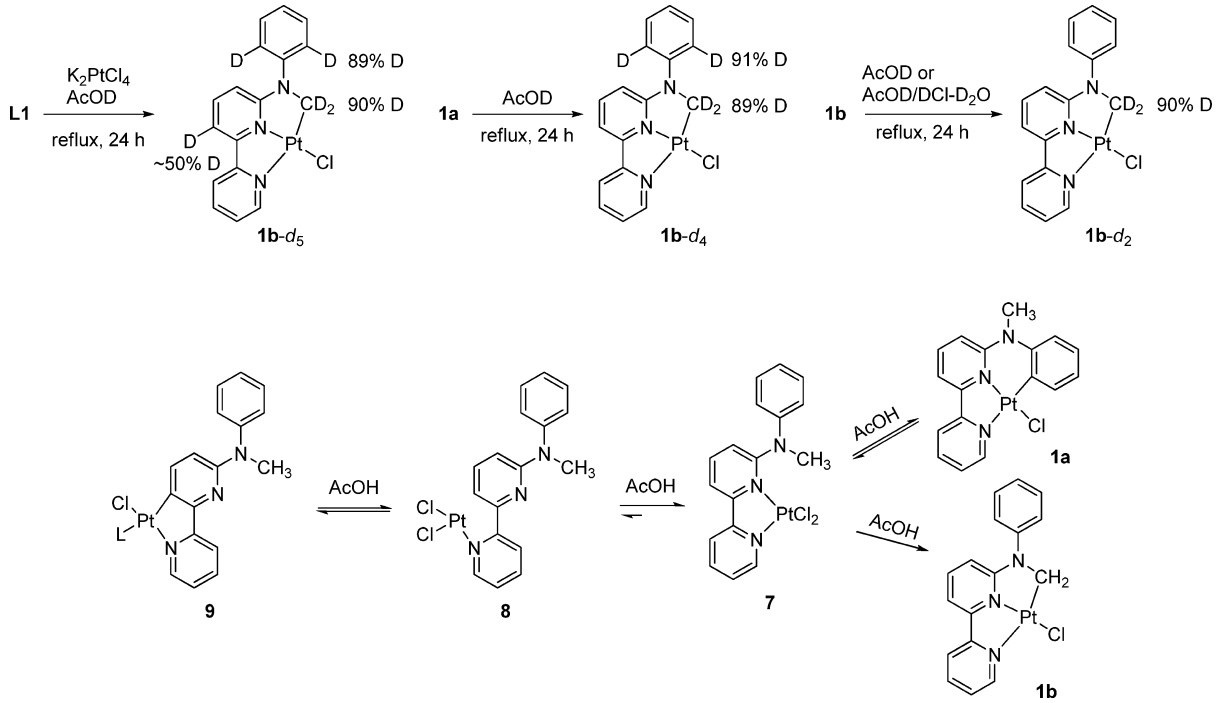

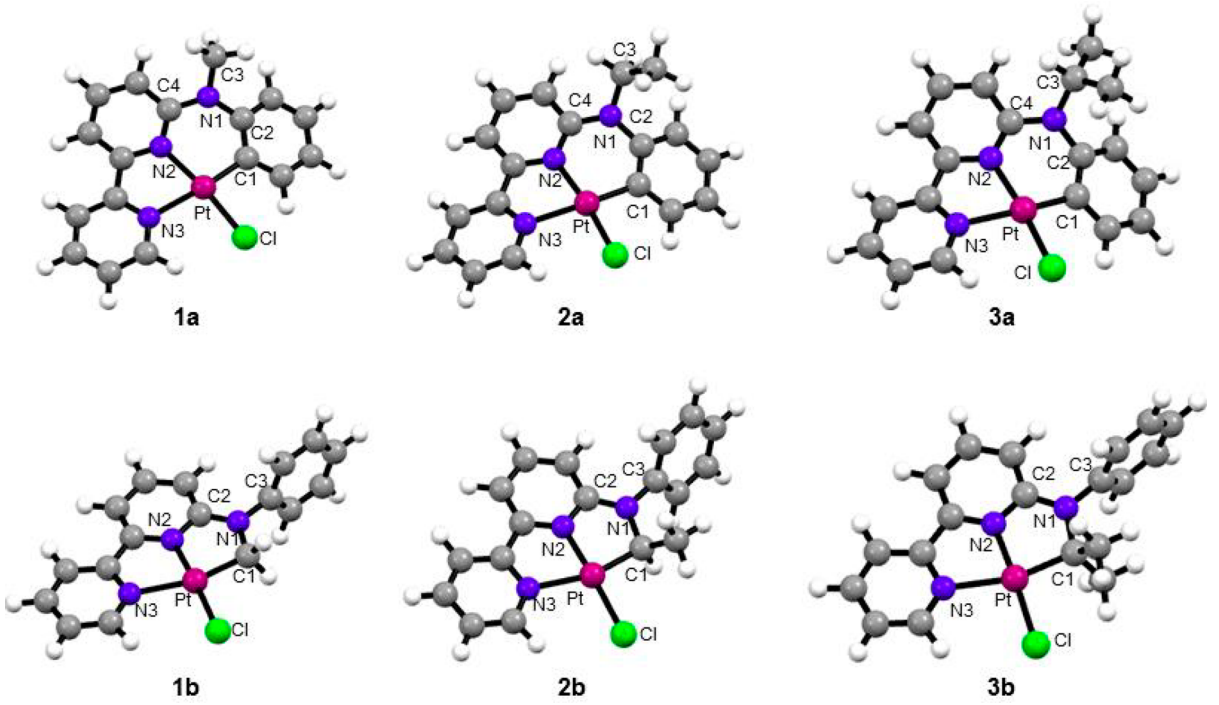

Figure 1. Optimized geometries of **1a**–**3a** and **1b**–**3b**.

tool to study the relative stability of the compounds. Moreover, compounds **4b**, **5a**, and **6b** were not formed; thus no experimental information on the structure and stability of these compounds was available. Therefore, we decided to conduct a systematic study on 12 possible cycloplatinated compounds from the cycloplatination of **L1**–**L6** using DFT calculations to elucidate the molecular structures and estimate the relative stability of the isomeric complexes.

DFT Calculations on Compounds 1a–3a and 1b–3b. *Geometric Optimization of 1a–3a and 1b–3b.* Although the X-ray structures of **3a** and **3b** have been reported,[1a] a systematic study on the geometry and stability of this series of platinum complexes is necessary to understand the selectivity of the reaction. In particular, a systematic change in the *N*-alkyl groups from methyl to isopropyl provides an excellent model to assess the steric effect of the alkyl group on the geometry and stability of these cyclometalated platinum compounds. Since the structures of **3a** and **3b** have been determined by X-ray crystallography, their structural parameters were used as the starting point of the optimization. Figure 1 shows optimized

DOI: 10.1021/acs.organomet.5b00326
Organometallics XXXX, XXX, XXX–XXX

Table 1. Optimized Bond Lengths (Å), Bond Angles (deg), and Torsional Angles (deg) of 1a−3a and 1b−3b

	1a			2a			3a			
	gas state	in MeCN	in AcOH	gas state	in MeCN	in AcOH	gas state	in MeCN	in AcOH	X-ray[1a]
Pt−Cl	2.332	2.372	2.362	2.330	2.371	2.362	2.328	2.373	2.363	2.310
Pt−C(1)	1.963	1.970	1.967	1.962	1.968	1.966	1.959	1.965	1.964	1.997
Pt−N2	2.038	2.026	2.030	2.041	2.026	2.030	2.045	2.029	2.032	2.000
Pt−N3	2.174	2.176	2.178	2.178	2.179	2.179	2.182	2.179	2.180	2.091
N1−C2	1.438	1.429	1.431	1.438	1.431	1.433	1.438	1.431	1.433	1.431
N1−C3	1.458	1.462	1.461	1.470	1.472	1.472	1.489	1.491	1.490	1.503
N1−C4	1.367	1.374	1.372	1.368	1.375	1.374	1.369	1.374	1.373	1.375
C(1)−Pt−N3	168.3	168.3	167.9	167.0	167.2	167.1	165.8	166.8	166.7	167.3
Cl−Pt−N3	92.6	93.0	93.0	93.2	93.6	93.5	93.2	93.2	93.2	93.1
Cl−Pt−C(1)	95.4	95.1	95.2	95.4	95.1	95.1	95.6	95.3	95.4	94.7
C(1)−Pt−N2	93.5	93.0	93.1	93.1	92.7	92.8	93.1	92.7	92.8	91.7
N2−Pt−N3	79.1	79.4	79.3	78.9	79.2	79.1	78.9	79.5	79.4	80.7
N2−Pt−Cl	170.7	171.4	171.1	171.2	172.0	171.8	170.7	171.5	171.3	173.5
C2−N1−C3	116.9	117.2	117.1	117.9	118.3	118.2	118.9	120.0	119.8	120.9
C3−N1−C4	116.7	116.6	116.7	117.8	117.6	117.6	116.5	116.4	116.4	115.6
C2−N1−C4	125.5	124.6	125.8	123.8	122.9	123.1	123.7	123.6	123.7	123.0
	1b			2b			3b			
	gas state	in MeCN	in AcOH	gas state	in MeCN	in AcOH	gas state	in MeCN	in AcOH	X-ray[1a]
Pt−Cl	2.332	2.383	2.372	2.336	2.387	2.376	2.341	2.390	2.380	2.303
Pt−C(1)	1.983	1.990	1.989	1.990	1.996	1.995	2.002	2.009	2.008	2.026
Pt−N2	1.963	1.957	1.958	1.963	1.956	1.957	1.961	1.956	1.957	1.944
Pt−N3	2.212	2.216	2.216	2.216	2.222	2.221	2.221	2.230	2.223	2.115
N1−C(1)	1.502	1.493	1.495	1.518	1.509	1.511	1.535	1.525	1.528	1.543
N1−C2	1.347	1.348	1.347	1.350	1.352	1.351	1.348	1.349	1.349	1.344
N1−C3	1.426	1.429	1.428	1.425	1.427	1.427	1.430	1.432	1.431	1.432
C(1)−Pt−N3	161.9	161.8	161.8	162.5	162.4	162.4	162.9	162.7	162.8	163.1
Cl−Pt−N3	99.1	100.3	100.1	99.1	100.0	99.7	99.3	99.8	99.6	99.9
Cl−Pt−C(1)	99.0	97.9	98.1	98.5	97.7	97.9	97.8	97.5	97.6	96.5
C(1)−Pt−N2	84.4	84.0	84.1	84.9	84.5	84.6	85.5	85.1	85.2	84.4
N2−Pt−N3	77.5	77.8	77.7	77.6	77.9	77.8	77.4	77.6	77.6	79.3
N2−Pt−Cl	176.6	178.1	177.8	176.6	177.8	177.5	176.7	177.9	177.2	178.3
C2−N1−C3	119.3	119.2	119.2	119.3	119.1	119.2	120.6	120.7	120.7	119.6
C2−N1−C(1)	121.0	121.4	121.3	121.0	121.3	121.2	119.1	119.3	119.2	118.9
C(1)−N1−C3	119. 7	119.4	119.4	119.8	119.5	119.6	120.2	120.0	120.0	121.0

geometries of **1a−3a** and **1b−3b** in their gas state. The major bond parameters around the coordination center and the amino nitrogen center for the optimized geometries in both the gas state and solvated states are listed in Table 1. The bond parameters from the X-ray crystal structures of **3a** and **3b** are also listed for comparison. Major bond lengths and angles for optimized geometries of **3a** and **3b** compare favorably with those determined by X-ray crystallography. It should be noted that the optimized geometry is for the molecule in its gas phase and solvated state, while the X-ray crystallography determines the solid-state structure. Therefore, small variations on the geometry in different states are expected. Nonetheless, the results suggest that the DFT method used here is very reliable in predicting the molecular geometry of the platinum complexes. The geometries of the compounds at their solvated states display a longer Pt−Cl bond distance by 0.04 and 0.05 Å in MeCN and 0.03 and 0.04 Å in AcOH compared with those in their gas states for **1a−3a** and **1b−3b**, respectively. This can be reasoned by the polarity of the Pt−Cl bond, because solvation assists the dissociation of a polar bond by stabilizing the charged species. Changes to the other bonds vary and are insignificant.

Complexes of platinum(II) with four ligands prefer a square planar geometry. When the four ligands are different, the square geometry may be distorted as the bond lengths between the platinum and the donor atoms of the ligands and bite angles of the ligands can be different, but a planar geometry is generally retained to maintain the efficient bonding between the metal center and the donor ligands, particularly those with extended conjugation. However, other factors such as torsional and angle strain may force the platinum coordination out of an ideal plane. Comparison between isomeric compounds **a** and **b** reveals that the coordination in complexes **1a−3a** is significantly deviated from a planar geometry, while the coordination geometry in **1b−3b** is nearly a perfect plane. Figure 2 displays the views of compounds **1a−3a** and **1b−3b** by projecting through the platinum coordination plane.

In **1b−3b**, the chlorine, the platinum, the carbon donor C1, the bipyridyl ring, and the linker amino nitrogen N1 are coplanar, as shown in Figure 2. The mean planes composed of the 12 atoms of the bipyridyl ring were calculated for **1a−3a** and **1b−3b**, and the deviations of the atoms from the plane are listed in Table 2. Also listed in Table 2 are the deviations of Pt, Cl, the amino nitrogen (N(1)), and the metalated carbon (C(1)) from the bipyridyl plane. In **3b** and **1b**, the

DOI: 10.1021/acs.organomet.5b00326
Organometallics XXXX, XXX, XXX−XXX

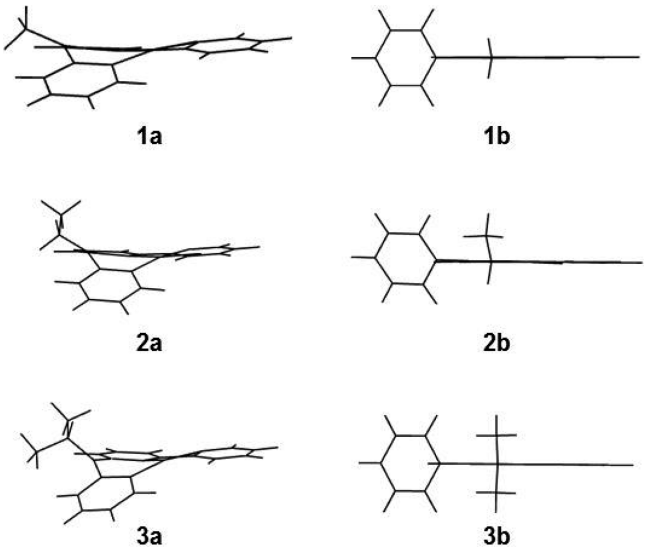

Figure 2. View of molecules by projecting through the bipyridyl ring in **1b**−**3b** and **1a**−**3a**.

Table 2. Deviations (Å) of Platinum, Chlorine, Amino Nitrogen N(1), Metalated Carbon C(1), Carbon, and Nitrogen Atoms in the Bipyridyl Ring from the Mean Plane of the Bipyridyl Ring

atom	1a	1b	2a	2b	3a	3b
Pt[a]	**0.273**	0.000	**0.299**	0.021	**0.251**	0.001
Cl[a]	**0.161**	0.000	**0.229**	0.067	**0.014**	0.001
C(1)[a]	**0.871**	0.000	**0.960**	0.024	**0.968**	0.003
N1[a]	0.0027	0.000	0.022	0.022	0.177	0.000
C_{py}[b]	0.058	0.000	0.053	0.016	0.119	0.000
C_{py}	0.090	0.000	0.081	0.013	0.106	0.000
C_{py}	0.142	0.000	0.139	0.019	0.210	0.000
C_{py}	0.071	0.000	0.077	0.004	0.109	0.000
C_{py}	0.090	0.000	0.087	0.008	0.107	0.000
C_{py}	0.071	0.000	0.066	0.004	0.080	0.000
C_{py}	0.150	0.000	0.147	0.014	0.207	0.000
C_{py}	0.061	0.000	0.063	0.009	0.109	0.000
C_{py}	0.100	0.001	0.093	0.007	0.114	0.000
C_{py}	0.146	0.001	0.143	0.017	0.208	0.000
N2	0.182	0.000	0.183	0.018	0.238	0.000
N3	0.061	0.000	0.066	0.011	0.112	0.000

[a]Not included in calculating the mean coordination planes in **1a**−**3a**. [b]C_{py} denotes carbon atoms in the bipyridyl ring.

coordination plane is perfect. The largest deviation was found to be only 0.003 Å in **3b**. The coordination geometry in **2b** is slightly deviated from a perfect plane, with the largest deviation of 0.043 Å. The phenyl ring in **1b**, **2b**, and **3b** is nearly perpendicular to the coordination plane, with dihedral angles of 89.95°, 65.71°, and 89.86°, respectively. The relatively small dihedral angle in **2b** may be attributed to the unsymmetrical spacious orientation of the methyl group repelling the phenyl ring and making it slightly twisted from a perpendicular orientation. The steric repulsion between the phenyl ring and the methyl group(s) can be seen clearly from small but distinct changes in angles C1−N−C3, C2−N−C3, and C1−N−C2 from **1b** to **2b** and to **3b**. As the number of methyl groups increases from zero in **1b** to two in **3b**, the steric hindrance increases. As a consequence, C1−N−C3 angles increase and C2−N−C3 angles decrease, while C1−N−C2 angles stay constant. In other words, the phenyl group is pushed away from the methyl group(s). The perpendicular orientation adopted by the phenyl ring is apparently to minimize the steric strain. Another consequence of the increasing steric interaction of the methyl group(s) is the stretching of the sp^3 C−N bond, which elongates gradually from 1.502 Å in **1b** to 1.518 and 1.535 Å in **2b** and **3b**, respectively. For the same reason, the C−Pt bond increases from 1.983 Å in **1b** to 2.002 Å in **3b**. The amino nitrogen adopts a perfect trigonal planar geometry, and the trigonal plane is coplanar with the bipyridyl ring with dihedral angles of 0.02°, 1.74°, and 0.07° for **1b**−**3b**, respectively.

The geometry of **1a** to **3a** is far from coplanar, showing significant bending of the phenyl ring relative to the platinum coordination plane and even twisting and bending of the two pyridyl rings (Figure 2). The dihedral angle of two pyridyl rings is 12.78°, 12.53°, and 17.87° for **1a**−**3a**, respectively. The dihedral angle between the phenyl ring and the bipyridyl ring is 31.19°, 35.86°, and 36.45° in **1a**, **2a**, and **3a**, respectively. The platinum and chlorine are approximately coplanar with the bipyridyl ring with a <0.3 Å deviation; however, the metalated carbons are severely deviated from the pyridyl plane, with a distance of 0.871, 0.960, and 0.968 Å in **1a**−**3a**, respectively.

The amino nitrogen (N1) adopts a slightly distorted trigonal planar geometry. The distance between the nitrogen and the trigonal plane composed of the three carbon atoms that bond to the nitrogen is 0.077, 0.056, and 0.078 Å for **1a**, **2a**, and **3a**, respectively. The dihedral angles between the trigonal plane and the bipyridyl ring are 32.51°, 38.85°, and 44.35° for **1a**−**3a**, respectively. The amino nitrogen deviates from the pyridyl plane by 0.027, 0.022, and 0.177 Å in **1a**, **2a**, and **3a**, respectively.

The distorted geometry of **1a**−**3a** contrasts sharply to **1b**−**3b**. One factor that should be considered is the different fused metallacycles. The former has a five−six fused metallacycle, while the latter has a five−five fused ring. The different size of the fused rings and nature of the C−Pt and N−Pt bonds may induce different angle strain. The steric effect incurred by the *N*-alkyl groups is perhaps the major contribution to the distorted geometry of **1a**−**3a**, as other similar molecules with a five−six fused metallacycle and a *N*-phenyl group rather than a *N*-alkyl group show a geometry much closer to a plane[15] because the *N*-phenyl ring can take a perpendicular orientation to avoid the steric interaction as mentioned above.

Relative Stability of the Isomeric Platinum Compounds. The calculated energies of the optimized geometries are

Table 3. Solvation Energies (ΔE_{sol} in kcal/mol) and Energy Differences (ΔE) between Isomeric sp^2/sp^3 C−H Bond Activation Products 1a,b−3a,b

	ΔE_{sol} (1a)	ΔE_{sol} (1b)	ΔE (1b−1a)	ΔE_{sol} (2a)	ΔE_{sol} (2b)	ΔE (2b−2a)	ΔE_{sol} (3a)	ΔE_{sol} (3b)	ΔE (3b−3a)
gas state			−2.19			−5.65			−8.26
In MeCN	−16.92	−15.51	−0.78	−16.79	−14.85	−3.71	−16.36	−14.18	−6.08
In AcOH	−13.17	−12.29	−1.31	−12.94	−11.62	−4.33	−12.61	−11.10	−6.75

DOI: 10.1021/acs.organomet.5b00326
Organometallics XXXX, XXX, XXX−XXX

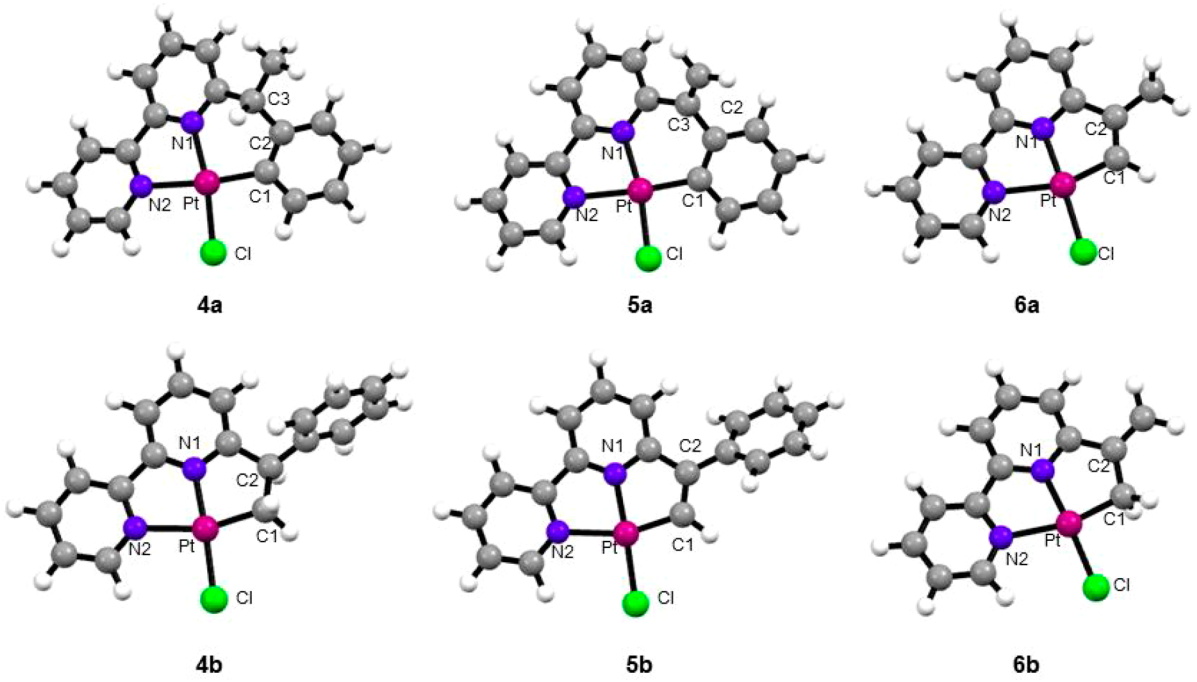

Figure 3. Optimized geometries of **4a**–**6a** and **4b**–**6b**.

Table 4. Optimized Bond Lengths (Å), Bond Angles (deg), and Torsional Angles (deg) of 4a–6a and 4b–6b

	4a			5a			6a		
	gas state	in MeCN	in AcOH	gas state	in MeCN	in AcOH	gas state	in MeCN	in AcOH
Pt–Cl	2.321	2.361	2.351	2.324	2.361	2.353	2.318	2.369	2.358
Pt–C(1)	1.976	1.979	1.978	1.974	1.979	1.978	1.941	1.951	1.949
Pt–N1	2.045	2.035	2.038	2.048	2.039	2.041	1.971	1.968	1.968
Pt–N2	2.196	2.196	2.197	2.190	2.190	2.190	2.226	2.234	2.231
C(1)–Pt–N2	165.3	164.8	164.9	168.3	168.0	168.0	159.4	159.5	159.5
Cl–Pt–N2	94.1	94.8	94.8	92.9	93.5	93.4	99.8	101.0	100.7
Cl–Pt–C(1)	95.1	94.6	94.6	94.8	94.3	94.5	100.8	99.5	99. 9
C(1)–Pt–N1	93.3	92.8	92.9	94.5	94.1	94.2	81.8	81.7	81.7
N1–Pt–N2	77.8	78.1	78.0	78.2	78.5	78.4	77.6	77.8	77.7
N1–Pt–Cl	171.6	172.6	172.5	170.5	171.3	171.1	177.4	178.8	178.4
	4b			**5b**			**6b**		
	gas state	in MeCN	in AcOH	gas state	in MeCN	in AcOH	gas state	in MeCN	in AcOH
Pt–Cl	2.322	2.376	2.364	2.316	2.368	2.357	2.324	2.376	2.365
Pt–C(1)	1.995	2.000	2.000	1.935	1.943	1.941	2.000	2.006	2.004
Pt–N1	1.974	1.971	1.972	1.973	1.970	1.970	1.972	1.970	1.970
Pt–N2	2.227	2.227	2.229	2.221	2.224	2.223	2.216	2.221	2.220
C1–C2	1.562	1.561	1.561	1.370	1.367	1.367	1.526	1.525	1.526
C2–C3	1.513	1.514	1.513	1.484	1.484	1.484	1.340	1.340	1.340
C2–C4	1.514	1.513	1.513	1.467	1.473	1.472	1.483	1.481	1.482
C(1)–Pt–N2	161.8	161.9	161.7	159.7	159.8	159.8	162.4	162.3	162.3
Cl–Pt–N2	99.1	100.0	99.8	99.6	101.0	100.7	98.9	99.9	99.8
Cl–Pt–C(1)	98.6	97.7	98.0	100.7	99.2	99.6	98.4	97.6	97.6
C(1)–Pt–N1	84.6	84.3	84.3	81.8	81.7	81.7	84.8	84.5	84.6
N1–Pt–N2	77.6	78.0	77.9	77.9	78.1	78.1	77.9	78.1	78.1
N1–Pt–Cl	176.8	177.9	177.6	177.4	178.7	178.4	176. 8	177.8	177.8
C1–C2–C3	114.1	113.2	113.6	123.9	123.7	123.8	124.6	124.5	124.5
C3–C2–C4	112.9	113.4	113.3	121.4	121.7	121.6	120.9	120.9	120.8
C1–C2–C4	110.6	110.3	110.3	114.7	114.6	114.7	114.5	114.5	114.6

corrected with zero-point energies. The solvation energy and the relative stability of isomers are summarized in Table 3. The solvation energy is expressed as the energy difference between those in the gas and solvated states, $\Delta E_{sol} = E_{sol} - E_{gas}$, with a negative value indicating a stabilization effect, where E_{sol} is the calculated energy of the molecule in its solvated state and E_{gas} is the energy of the molecule in its gas state. The relative stability of isomers is expressed as the energy difference between the

DOI: 10.1021/acs.organomet.5b00326
Organometallics XXXX, XXX, XXX–XXX

two isomers **b** and **a**, $\Delta E = E_b - E_a$. The results can be summarized as follows. First, in both the gas phase and the solvated state, all the sp^3 C−H activation products **1b**, **2b**, and **3b** are predicted to be more stable than their isomeric sp^2 C−H activation products **1a**, **2a**, and **3a**, respectively, and the energy difference between the two isomers increases with the increasing size of the *N*-alkyl groups from methyl (**1a** and **1b**) to ethyl (**2a** and **2b**) to isopropyl (**3a** and **3b**). These results are consistent with the experimental finding that **1b**−**3b** are the thermodynamic products and **1a**−**3a** are kinetic products.[1] Second, solvents significantly stabilize the cyclometalated complexes (by 11−17 kcal/mol), and the stabilization slightly decreases from **1a** and **1b** to **3a** and **3b**. Acetonitrile stabilizes the complexes by about 3−4 kcal/mol more than acetic acid does. Finally, the solvent stabilization on **1a**, **2a**, and **3a** is slightly higher than that on **1b**, **2b**, and **3b**, by about 1−2 kcal/mol.

The greater stability of **1b**−**3b** can be reasoned by their planar coordination geometry, which maximizes the electron delocalization stabilization through conjugation between the bipyridyl ring, the amino, and the platinum center.

DFT Calculations on 4a−6a and 4b−6b. *Geometric Optimization of 4a−6a and 4b−6b.* The optimized geometries are shown in Figure 3. The structural parameters around the coordination sphere of optimized geometries including both the gas state and the solvated states are listed in Table 4. It can be seen from the table that the geometries of the compounds in their solvated states display a longer Pt−Cl bond distance compared with those in their gas states by 0.05 and 0.04 Å in MeCN and AcOH, respectively. The changes to other bonds are not significant. The mean plane of the bipyridyl ring is calculated, and the deviations of the atoms from the plane are listed in Table 5. Also listed are the deviations of other atoms in the coordination sphere. Figure 4 shows the view of molecular structures of **4a**−**6a** and **4b**−**6b** by projecting through the plane of the bipyridyl ring. Compound **4a** has a fused five−six-membered metallacyle and displays a significantly distorted geometry from a planar coordination. Even the bipyridyl ring is slightly twisted and bent, with the dihedral angle between the two pyridyl rings being 8.52°. The platinum, chlorine, and the carbon donor C(1) are deviated from the bipyridyl ring by 0.540, 0.782, and 1.275 Å, respectively. The dihedral angle between the phenyl ring and the bipyridyl ring is 49.42°. The six-membered metallacyle adopts a boat-like conformation. In **4b**, the bipyridyl ring is planar, and Pt, Cl, carbon donor C(1), and the linking carbon atom C(2) deviate from the plane by 0.138, 0.281, 0.365, and 0.147 Å, respectively. The platinum forms a stronger C−Pt bond in **4a** than that in **4b**, presumably due to the nature of the carbon donors: an sp^2 carbon normally forms a stronger bond than an sp^3 carbon.

Table 5. Deviations (Å) of Platinum, Chlorine, Carbon, and Nitrogen Atoms in the Bipyridyl Ring from the Mean Plane of the Bipyridyl Ring

atom	4a	4b	5a	5b	6a	6b
Pt[a]	0.504	0.138	0.400	0.026	0.000	0.095
Cl[a]	**0.782**	0.281	0.504	0.104	0.000	0.176
C(1)[a]	**1.275**	0.365	**1.052**	0.013	0.001	**0.266**
C2[a]	0.902	0.167	0.144	0.020	0.001	0.084
C3[a]	0.277	0.410	**1.090**	0.048	0.002	**0.507**
C_{py}[b]	0.051	0.023	0.014	0.023	0.001	0.015
C_{py}	0.120	0.013	0.101	0.011	0.000	0.007
C_{py}	0.050	0.006	0.079	0.024	0.001	0.001
C_{py}	0.024	0.008	0.011	0.009	0.000	0.001
C_{py}	0.101	0.013	0.090	0.007	0.000	0.011
C_{py}	0.072	0.007	0.068	0.003	0.000	0.006
C_{py}	0.053	0.005	0.085	0.019	0.001	0.003
C_{py}	0.033	0.013	0.002	0.015	0.000	0.005
C_{py}	0.093	0.008	0.091	0.006	0.001	0.008
C_{py}	0.055	0.004	0.085	0.023	0.000	0.004
N1	0.018	0.015	0.145	0.022	0.000	0.018
N2	0.134	0.008	0.009	0.017	0.000	0.003

[a]Not included in calculating the mean coordination planes. [b]C_{py} denotes carbon atoms in the bipyridyl ring.

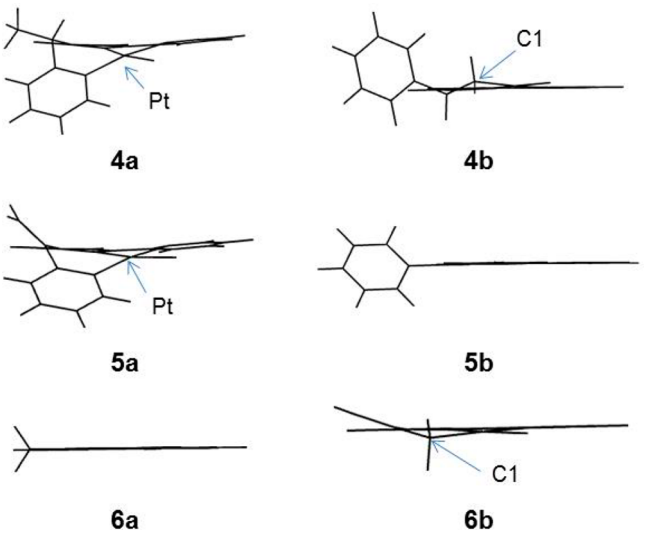

Figure 4. Molecular view of **4a**−**6a** and **4b**−**6b** by projecting through the bipyridyl ring.

The coordination geometry in compound **5a** is also severely distorted from a plane. It is interesting to note that the geometries of **4a** and **5a** are very similar to each other (Figures 3 and 4), although the linking atom between the bipyridyl and the phenyl rings is an sp^3 carbon in **4a** but an sp^2 carbon in **5a**. The bipyridyl ring is also twisted and bent (dihedral angle of 8.92°). The platinum, chlorine, and the carbon donor C(1) deviate from the bipyridyl ring by 0.400, 0.504, and 1.052 Å, respectively. The dihedral angle between the phenyl and the bipyridyl rings is 37.25°. The vinyl group is bent with respect to the bipyridyl plane with the terminal vinyl carbon deviated by 1.090 Å. The vinyl group maintains a planar geometry, but forms a dihedral angle of 44.46° and 49.27° with the phenyl ring and the bipyridyl ring, respectively. Such significant deviation from the planar geometry is likely the result of balance between steric interaction (Chart 3) and electron delocalization. On the contrary, compound **5b**, with metalation at the vinyl carbon, displays nearly perfect planar coordination geometry. The chlorine shows the largest deviation from the bipyridyl plane, but by only 0.1 Å. The phenyl ring adopts a twisted orientation, forming a dihedral angle of 49.91° with the coordination plane to minimize the steric interaction. The C−Pt bond in compound **5b** is also stronger than that of **5a** (1.935 vs 1.974 Å), even though both are sp^2 C−Pt bonds.

Compound **6a** has perfect planar coordination geometry, but its isomer **6b** shows distorted geometry because of steric interaction between the linking vinyl group and the bipyridyl group. The platinum in **6b** is only slightly deviated from the

DOI: 10.1021/acs.organomet.5b00326
Organometallics XXXX, XXX, XXX−XXX

Table 6. Solvation Energies (ΔE_{sol} in kcal/mol) and Energy Differences (ΔE) between Isomeric C−H Bond Activation Products 4a,b−6a,b

	ΔE_{sol} (4a)	ΔE_{sol} (4b)	ΔE (4b−4a)	ΔE_{sol} (5a)	ΔE_{sol} (5b)	ΔE (5b−5a)	ΔE_{sol} (6a)	ΔE_{sol} (6b)	ΔE (6b−6a)
gas state			2.86			−3.56			6.98
in MeCN	−16.89	−16.93	2.83	−16.81	−15.79	−2.54	−15.20	−16.11	6.07
in AcOH	−13.11	−13.28	2.70	−13.04	−12.40	−2.92	−11.89	−12.66	6.22

bipyridyl ring, by 0.095 Å, but the chlorine and the metalated carbon C(1) show a 0.176 and 0.266 Å distance to the plane, respectively. The planar vinyl group is bent from the bipyridyl plane with the terminal vinyl carbon distanced by 0.507 Å and forms a dihedral angle of 18.59° with the bipyridyl ring. The C−Pt bond in **6a** (1.941 Å) is much shorter than that in **6b** (2.000 Å), indicative of stronger bonding in **6a**.

Relative Stability of Isomeric Cycloplatinated Compounds. The energies of the optimized geometries were corrected with zero-point energies. The solvent energies and the energy differences between isomeric compounds are summarized in Table 6. In both the gas phase and solvated state, compounds **4a**, **5b**, and **6a** are predicted to be more stable than their isomers **4b**, **5a**, and **6b**, respectively, which are consistent with the experimental finding that **4a**, **5b**, and **6a** are formed exclusively as likely thermodynamic products. Solvents significantly stabilize the cyclometalated complexes (by 11−17 kcal/mol), and acetonitrile stabilizes the complexes by about 3−4 kcal/mol more than acetic acid does.

The greater stability of **5b** and **6a** can be attributed to the planar geometry of the coordination compounds, which maximizes the bonding and electron delocalization, particularly the conjugation between the vinyl group and the bipyridyl ring. It is also conceivable that the five-membered platinacycle in **5b** and **6a** may possess aromatic character.[16] The larger difference between **6a** and **6b** may be attributed to the stronger vinyl C−Pt bonding in **6a** that adds additional stabilization. On the other hand, both **4a** and **4b** have a twisted geometry, but **4a** is calculated to be more stable than **4b** by 2.86 kcal/mol in the gas state. This is at least partially due to the stronger sp^2 C−Pt bonding in **4a** than the sp^3 C−Pt in **4b**.

SUMMARY

In the cycloplatintion of 6-substituted 2,2′-bipyridines where competing sp^2/sp^3 or vinyl/aryl C−H bond activation is involved, the outcome of the reaction varies depending on the structure of the 6-substituents. In the reaction of *N*-alkyl-*N*-phenyl-2,2′-bipyridin-6-amine (alkyl = methyl (**L1**), ethyl (**L2**), and isopropyl (**L3**)), the selectivity of competing sp^2/sp^3 C−H bond activation can be controlled by using different solvents, resulting in either thermodynamic or kinetic control of the reaction. DFT calculations predict that the products **1b−3b** via the sp^3 C−H activation are more stable than their corresponding isomers **1a−3a** via the sp^2 C−H activation, which confirms the thermodynamic control of the reaction in acetic acid. On the other hand, the reactions of 6-(1-phenylethyl)-2,2′-bipyridine (**L4**), 6-(1-phenylvinyl)-2,2′-bipyridine (**L5**), and 6-(prop-1-en-2-yl)-2,2′-bipyridine (**L6**) produce exclusively **4a**, **5b**, and **6a**, respectively, via sp^2 or vinyl C−H activation. DFT calculations indicate that these compounds are more stable than their isomers via the other competing C−H activation. The formation of the sole product is most likely both kinetically and thermodynamically controlled. We are currently performing a DFT calculation to simulate the reaction pathways of cycloplatination of **L1** and elucidating the transition states and intermediates in the reaction, and the results will be reported in due course.

EXPERIMENTAL SECTION

Synthesis. All reactions involving moisture- and/or oxygen-sensitive organometallic complexes were carried out under a nitrogen or argon atmosphere and anhydrous conditions. Tetrahydrofuran (THF) and diethyl ether were distilled from sodium and benzophenone under nitrogen before use. All other anhydrous solvents were purchased from Aldrich Chemical Co. and were used as received. 6-Bromo-2,2′-bipyridine[17] was prepared according to the literature procedure. All other reagents were purchased from chemical companies and were used as received. NMR spectra were measured on a Bruker 400 or a Varian 500 spectrometer. Spectra were taken in $CDCl_3$ or CD_2Cl_2 using tetramethylsilane as standard for ^{1}H NMR chemical shifts and the solvent peak ($CDCl_3$, 77.0 ppm; CD_2Cl_2, 53.8 ppm) as standard for ^{13}C NMR chemical shifts. Coupling constants (J) are reported in Hz. The 2D COSY experiments were performed using standard pulse sequences. Elemental analyses were performed at Atlantic Microlab, Inc., Norcross, GA, USA.

*Preparation of **L4**.* A 50 mL three-neck round-bottom flask was charged with LiCl (0.42 g, 10 mmol) and Zn dust (0.65 g, 10 mmol), dried with a heat gun under vacuum, and backfilled three times with argon. Tetrahydrofuran (3 mL) and 1,2-dibromoethane (22 μL, 0.25 mmol) were added, and the mixture was heated at 60 °C for 20 min. After cooling to room temperature, TMSCl (6.3 μL, 0.05 mmol) and iodine (3.2 mg, 0.025 mmol) in a THF solution were added. This mixture was heated at 60 °C for 20 min and then cooled to room temperature, followed by addition of 1-bromoethylbenzene (0.68 mL, 5 mmol). The mixture was stirred at 50 °C for 16 h. In a separate argon-flushed 50 mL three-neck round-bottom flask, 6-bromo-2,2′-bipyridine (0.47 g, 2 mmol), $PdCl_2$(dppf) (82 mg, 0.1 mmol), and THF (2 mL) were added. The supernatant of the Zn reagent mixture was added dropwise to the reaction flask, and the reaction mixture was heated at 50 °C for 3 h. After quenching with 20 mL of water, EDTA (5.8 g, 20 mmol), and Na_2CO_3 (4.2 g, 40 mmol), the organic products were extracted with 3 × 75 mL portions of ethyl acetate and the combined organic layers were washed with brine and dried over $MgSO_4$. Solvent was removed by rotary evaporation, and the crude product was purified by column chromatography on silica gel with hexane and ethyl acetate (v/v 5/1): yellow-brown oil, 0.34 g, 65%. ^{1}H NMR (400 MHz, $CDCl_3$): δ 8.66 (d, J = 4.8, 1 H), 8.53 (d, J = 8.0, 1 H), 8.21 (d, J = 7.9, 1 H), 7.82 (td, J = 7.8, 1.8, 1 H), 7.68 (t, J = 7.8, 1 H), 7.37 (m, 2 H), 7.30 (m, 3 H), 7.20 (t, J = 7.4, 1 H), 7.10 (d, J = 7.7, 1 H), 4.35 (q, J = 7.3, 1 H), 1.78 (d, J = 7.2, 3 H).

*Preparation of **L5**.* A 50 mL three-neck round-bottom flask under argon was cooled to −78 °C and charged with diethyl ether (3 mL) and α-bromostyrene (0.25 mL, 2 mmol). The resulting brown mixture was stirred for 10 min, followed by dropwise addition of *t*-BuLi (1.7 M solution in pentane, 2.35 mL, 4 mmol). $ZnCl_2$ (1.0 M solution in ether, 1 mL, 1 mmol) was added dropwise, and the reaction mixture was stirred for 30 min before warming to room temperature. Next, 6-bromo-2,2′-bipyridine (235.1 mg, 1 mmol), $Pd(PPh_3)_4$ (57.8 mg, 0.05 mmol), and THF (8 mL) were added, and the mixture was heated at reflux for 3 h. After quenching with 20 mL of water, EDTA (292 mg, 1 mmol), and Na_2CO_3 (106 mg, 1 mmol), the organic products were extracted with three 30 mL portions of ethyl acetate and the combined organic layers were washed with brine and dried over $MgSO_4$. Solvent was removed by rotary vapor, and the crude product was purified by column chromatography on silica gel with hexane and ethyl acetate (v/v 5/1): yellow-brown solid, 0.22 g, 86%. ^{1}H NMR (400 MHz,

DOI: 10.1021/acs.organomet.5b00326
Organometallics XXXX, XXX, XXX−XXX

$CDCl_3$): δ 8.68 (d, J = 5.2, 1 H), 8.47 (d, J = 8.0, 1 H), 8.35 (d, J = 7.9, 1 H), 7.80 (td, J = 7.7, 1.8, 1 H), 7.76 (t, J = 7.8, 1 H), 7.39 (m, 5 H), 7.30 (m, 1 H), 7.26 (d, J = 7.8, 1 H), 6.25 (d, J = 1.7, 1 H), 5.64 (d, J = 1.7, 1 H). ^{13}C NMR (75 MHz, $CDCl_3$): δ 157.3, 156.3, 155.5, 149.0 (2 C), 140.5, 137.2, 136.9, 128.6 (2 C), 128.2 (2 C), 127.7, 123.7, 122.7, 121.3, 119.7, 117.9. HRMS (ESI-QToF): calcd for $C_{18}H_{15}N_2$ $(M + H)^+$ 259.12, found 259.03. Anal. Calcd for $C_{18}H_{14}N_2$: C, 83.69; H, 5.46; N, 10.84. Found: C, 83.42; H, 5.66; N, 10.79.

Preparation of ***L6***. A 100 mL three-neck round-bottom flask under argon was cooled to 0 °C and charged with isopropenyl magnesium bromide (0.5 M solution in THF, 12 mL, 6 mmol). Zinc chloride (1.0 M solution in ether, 6 mL, 6 mmol) was added dropwise, and the reaction mixture was stirred 15 min before warming to room temperature. Next, 6-bromo-2,2′-bipyridine (470 mg, 2 mmol) and $Pd(PPh_3)_4$ (116 mg, 0.1 mmol) were added, and the resulting cloudy, green mixture was heated at reflux for 19 h. After quenching with 20 mL of water, EDTA (3.4 g, 12 mmol), and Na_2CO_3 (5.1 g, 48 mmol), the organic products were extracted with three 30 mL portions of ethyl acetate and the combined organic layers were washed with brine and dried over $MgSO_4$. Solvent was removed by rotary vapor, and the crude product was purified by column chromatography on silica gel with hexane and ethyl acetate (v/v 5/1): yellow-brown oil, 0.32 g, 82%. ^{1}H NMR (400 MHz, $CDCl_3$): δ 8.66 (d, J = 4.8, 1 H), 8.53 (d, J = 8.0, 1 H), 8.31 (d, J = 7.8, 1 H), 7.81 (td, J = 7.8, 1.8, 1 H), 7.78 (t, J = 7.8, 1 H), 7.51 (d, J = 4.8, 1 H), 7.29 (m, 1 H), 6.00 (s, 1 H), 5.35 (s, 1 H), 2.30 (s, 3 H). ^{13}C NMR (75 MHz, $CDCl_3$): δ 157.4, 156.5, 154.9, 149.0, 143.4, 137.2, 136.8, 123.6, 121.2, 119.6, 119.2, 115.5, 20.5. HRMS (ESI-QToF): calcd for $C_{13}H_{13}N_2$ $(M + H)^+$ 197.11, found 197.09. Anal. Calcd for $C_{13}H_{12}N_2$: C, 79.56; H, 6.16; N, 14.27. Found: C, 79.04; H, 6.42; N, 14.23.

Reaction of ***L4*** *with* K_2PtCl_4 *in Acetic Acid: Preparation of* ***4a***. To a 50 mL round-bottom flask with condenser were added **L4** (130 mg, 0.5 mmol), K_2PtCl_4 (208 mg, 0.5 mmol), and glacial acetic acid (20 mL). The mixture was heated at reflux for 12 h, and then the yellow precipitate was collected by suction filtration. The crude product was purified by column chromatography on silica gel with dichloromethane and ethyl acetate (v/v 50/1): yellow solid, 0.18 g, 73%. ^{1}H NMR (400 MHz, $CDCl_3$): δ 9.70 (d, J = 5.4, H-6′), 8.10 (d, J = 7.6, $^3J_{Pt-H}$ = 47, H-6″), 8.04 (d, J = 7.4, H-4′), 7.97 (t, J = 7.8, H-4), 7.93 (d, J = 8.1, H-3′), 7.82 (d, J = 7.8, H-3), 7.62 (t, J = 6.4, H-5′), 7.49 (d, J = 8.0, H-5), 7.05 (m, 3 H, phenyl-H), 4.38 (q, J = 7.1, CH), 1.87 (d, J = 7.2, CH_3). ^{13}C NMR (75 MHz, DMSO-d_6): δ 164.2, 157.9, 155.5, 148.1, 142.5, 140.3, 139.9, 139.0, 130.1, 127.6, 126.7, 125.7, 124.9, 123.9, 123.6, 122.5, 54.5, 28.2.

Reaction of ***L4*** *with* K_2PtCl_4 *in Acetonitrile*. To a 50 mL round-bottom flask with condenser were added **L4** (130 mg, 0.5 mmol), K_2PtCl_4 (208 mg, 0.5 mmol), and acetonitrile (20 mL). The mixture was heated at reflux for 2 d, and then the solvent was removed by rotary evaporator. The crude product **4a** was purified by column chromatography on silica gel with dichloromethane and ethyl acetate (v/v 50/1): yellow solid, 73.1 mg, 30%.

Reaction of ***L5*** *with* K_2PtCl_4 *in Acetic Acid: Preparation of* ***5b***. To a 50 mL round-bottom flask with condenser were added **L5** (129 mg, 0.5 mmol), K_2PtCl_4 (208 mg, 0.5 mmol), and glacial acetic acid (20 mL). The mixture was heated at reflux for 17 h, and then 10 mL of water was added. The orange precipitate was collected using suction filtration, 170 mg, 70%. ^{1}H NMR (400 MHz, CD_2Cl_2): δ 8.97 (d, J = 5.4, $^3J_{Pt-H}$ = 13.4, H-6′), 8.13 (td, J = 7.9, 1.7, H-4′), 7.97 (d, J = 8.2, H-3′), 7.95 (s, $^2J_{Pt-H}$ = 57, 1 H), 7.75 (m, H-4 and H-5′), 7.55 (d, J = 7.9, $^4J_{Pt-H}$ = 13.2, H-3), 7.44 (m, 4 H, Phenyl-H), 7.37 (m, 1 H, Phenyl-H), 7.15 (d, J = 8.2, $^4J_{Pt-H}$ = 11.6, H-6). HRMS (ESI-QToF): calcd for acetonitrile complex, $C_{20}H_{16}N_3Pt$ $(M)^+$ 493.1, found 493.1. Anal. Calcd for $C_{18}H_{13}ClN_2Pt$: C, 44.32; H, 2.69; N, 5.74. Found: C, 44.03; H, 2.82; N, 5.74.

Reaction of ***L5*** *with* K_2PtCl_4 *in Acetonitrile*. To a 50 mL round-bottom flask with condenser were added **L4** (65 mg, 0.25 mmol), K_2PtCl_4 (104 mg, 0.25 mmol), and acetonitrile (20 mL). The mixture was heated at reflux for 3 d, and then the solvent was removed by rotary evaporator. The crude product **5b** was purified by column chromatography on silica gel with dichloromethane and ethyl acetate (v/v 1/1): orange solid, 94.4 mg, 79%.

Reaction of ***L6*** *with* K_2PtCl_4 *in Acetic Acid: Preparation of* ***6a***. To a 50 mL round-bottom flask with condenser were added **L6** (49 mg, 0.25 mmol), K_2PtCl_4 (104 mg, 0.25 mmol), and glacial acetic acid (12 mL). The mixture was heated at reflux for 2 h, resulting in a dark orange mixture with some black precipitate. The solvent was removed by rotary evaporator, and the crude product was purified by column chromatography on silica gel with dichloromethane: gold solid, 40.2 mg, 38%. ^{1}H NMR (400 MHz, CD_2Cl_2): δ 8.96 (d, J = 5.8, $^3J_{Pt-H}$ = 12.8, H-6′), 8.12 (td, J = 7.9, 1.6, H-4′), 7.94 (d, J = 7.9, H-3′), 7.80 (t, J = 7.9, H-4), 7.72 (dd, J = 7.7, 1.2, H-5′), 7.54 (s, $^2J_{Pt-H}$ = 60.6, vinyl-H), 7.50 (d, J = 8.0, H-3), 6.97 (d, J = 8.0, $^4J_{Pt-H}$ = 11.4, H-6), 2.09 (s, CH_3). HRMS (ESI-QToF): calcd for acetonitrile complex, $C_{15}H_{14}N_3Pt$ $(M)^+$ 431.1, found 431.1. Anal. Calcd for $C_{13}H_{11}ClN_2Pt$: C, 36.67; H, 2.60; N, 6.58. Found: C, 36.14; H, 2.61; N, 6.44.

Reaction of ***L6*** *with* K_2PtCl_4 *in Acetonitrile*. To a 50 mL round-bottom flask with condenser were added **L6** (49 mg, 0.25 mmol), K_2PtCl_4 (104 mg, 0.25 mmol), and acetonitrile (12 mL). The mixture was heated at reflux for 19 h, and then the solvent was removed by rotary evaporator and the crude product **6a** was purified by column chromatography on silica gel with dichloromethane: gold solid, 81.6 mg, 77%.

DFT Calculations. Geometry optimizations and energy calculations for the 12 possible cycloplatination products were carried out using the Gaussian 09 (G09) program[18] at density functional theory level with the M062X functional[19] and def2-TZVP basis set for Pt[20] and cc-pVDZ[21] for other atoms (M062X/def2-TZVP-Pt/cc-pVDZ). The solvent effects were simulated with the polarizable continuum model using the integral equation formalism variant (PCM).[22] The frequency calculation was performed for each compound at the optimized geometry at the same level of theory as used in optimization. All the computations in this work were completed at East Carolina University using the Altix 4700 computer cluster.

■ ASSOCIATED CONTENT

Ⓢ Supporting Information

NMR spectra of the ligands and the complexes. A text file of all computed molecule Cartesian coordinates in .xyz format for convenient visualization. The Supporting Information is available free of charge on the ACS Publications website at DOI: 10.1021/acs.organomet.5b00326.

■ AUTHOR INFORMATION

Corresponding Authors

*E-mail (Y. Li): liyu@ecu.edu.

*E-mail (S. Huo): huos@ecu.edu.

Notes

The authors declare no competing financial interest.

■ ACKNOWLEDGMENTS

Acknowledgment is made to the Donors of the American Chemical Society Petroleum Research Fund (#51147-UR3), for partial support of this research. J.C. is the recipient of a Burroughs-Wellcome fellowship.

■ REFERENCES

(1) (a) Garner, A. W.; Harris, C. F.; Vezzu, D. A. K.; Pike, R. D.; Huo, S. *Chem. Commun.* **2011**, *47*, 1902−1904. (b) Carroll, J.; Gagnier, J. P.; Garner, A. W.; Moots, J. G.; Pike, R. D.; Li, Y.; Huo, S. *Organometallic* **2013**, *32*, 4828−4836.

(2) For other examples of selective sp^2/sp^3 C−H bond activation by platinum, see: (a) Albert, J.; Ceder, R. M.; Gomez, M.; Granell, J.; Sales, J. *Organometallics* **1992**, *11*, 1536−1541. (b) Stoccoro, S.; Soro, B.; Minghetti, G.; Zucca, A.; Cinellu, M. A. *J. Organomet. Chem.* **2003**, *679*, 1−9. (c) Vazquez-Garcia, D.; Fernandez, A.; Lopez-Torres, M.;

DOI: 10.1021/acs.organomet.5b00326
Organometallics XXXX, XXX, XXX−XXX

Rodriguez, A.; Gomez-Blanco, N.; Viader, C.; Vila, J. M.; Fernandez, J. J. *Organometallics* **2010**, *29*, 3303−3307. (d) Crosby, S. H.; Clarkson, G. J.; Rourke, J. P. *J. Am. Chem. Soc.* **2009**, *131*, 14142−14143. (e) Thomas, H. R.; Deeth, R. J.; Clarkson, G. J.; Rourke, J. P. *Organometallics* **2011**, *30*, 5641−5648. (f) Crosby, S. H.; Clarkson, G. J.; Rourke, J. P. *Organometallics* **2011**, *30*, 3603−3609. (g) Crosby, S. H.; Deeth; Robert, J.; Clarkson, G. J.; Rourke, J. P. *Dalton Trans.* **2011**, *40*, 1227−1229. (h) Anderson, C. M.; Crespo, M.; Kfoury, N.; Weinstein, M. A.; Tanski, J. M. *Organometallics* **2013**, *32*, 4199−4207. (i) Cocco, F.; Zucca, A.; Stoccoro, S.; Serratrice, M.; Guerri, A.; Cinellu, M. A. *Organometallics* **2014**, *33*, 3414−3424.

(3) For examples of selective sp^2/sp^3 C−H bond activation by palladium, see: (a) Tamaru, Y.; Kagotani, M.; Yoshida, Z.-i. *Angew. Chem., Int. Ed. Engl.* **1981**, *20*, 980−981. (b) Albert, J.; Ceder, R. M.; Gomez, M.; Granell, J.; Sales, J. *Organometallics* **1992**, *11*, 1536−1541. (c) Alsters, P. L.; Engel, P. F.; Hogerheide, M. P.; Copijn, M.; Spek, A. L.; van Koten, G. *Organometallics* **1993**, *12*, 1831−1844. (d) Cardenas, D. J.; Echavarren, A. M.; Vegas, A. *Organometallics* **1994**, *13*, 882−889. (e) Dunina, V. V.; Golovan', E. B. *Inorg. Chem. Commun.* **1998**, *1*, 12−14. (f) Zucca, A.; Cinellu, M. A.; Pinna, M. V.; Stoccoro, S.; Minghetti, G.; Manassero, M.; Sansoni, M. *Organometallics* **2000**, *19*, 4295−4303. (g) Dunina, V. V.; Gorunova, O. N.; Averina, E. B.; Grishin, Y. K.; Kuz'mina, L. G.; Howard, J. A. K. *J. Organomet. Chem.* **2000**, *603*, 138−151. (h) Stoccoro, S.; Soro, B.; Minghetti, G.; Zucca, A.; Cinellu, M. A. *J. Organomet. Chem.* **2003**, *679*, 1−9. (i) Vazquez-Garcia, D.; Fernandez, A.; Lopez-Torres, M.; Rodriguez, A.; Gomez-Blanco, N.; Viader, C.; Vila, J. M.; Fernandez, J. J. *Organometallics* **2010**, *29*, 3303−3307.

(4) Houghton, R. P. *Metal Complexes in Organic Chemistry*; Cambridge University Press: London, UK, 1979; pp 61−62.

(5) Balcells, D.; Clot, E.; Eisenstein, O. *Chem. Rev.* **2010**, *110*, 749−823.

(6) (a) Rybtchinski, B.; Oevers, S.; Montag, M.; Vigalok, A.; Rozenberg, H.; Martin, J. M. L.; Milstein, D. *J. Am. Chem. Soc.* **2001**, *123*, 9064−9077. (b) Otto, S.; Chanda, A.; Samuleev, P. V.; Ryabov, A. D. *Eur. J. Inorg. Chem.* **2006**, 2561−2565. (c) Marrone, A.; Re, N.; Romeo, R. *Organometallics* **2008**, *27*, 2215−2222.

(7) Minghetti, G.; Cinellu, M. A.; Chelucci, G.; Gladiali, S.; Demartin, F.; Manassero, M. *J. Organomet. Chem.* **1986**, *307*, 107−114.

(8) Botteghi, C.; Chelucci, G.; Chessa, G.; Delogu, G.; Gladiali, S.; Soccolini, F. *J. Organomet. Chem.* **1986**, *304*, 217−225.

(9) Hayashi, T.; Konishi, M.; Kumada, M. *Tetrahedron Lett.* **1979**, 1871−1874.

(10) Metzger, A.; Schade, M. A.; Knochel, P. *Org. Lett.* **2008**, *10*, 1107−1110.

(11) Romeo, R.; Plutino, M. R.; Scolaro, L. M.; Stoccoro, S.; Minghetti, G. *Inorg. Chem.* **2000**, *39*, 4749−4755.

(12) Zucca, A.; Stoccoro, S.; Cinellu, M. A.; Minghetti, G.; Manassero, M.; Sansoni, M. *Eur. J. Inorg. Chem.* **2002**, 3336−3346.

(13) (a) Negishi, E.; King, A. O.; Okukado, N. *J. Org. Chem.* **1977**, *42*, 1821−1823. (b) King, A. O.; Okukado, N.; Negishi, E. *J. Chem. Soc., Chem. Commun.* **1977**, 683−684. (c) Negishi, E. *Acc. Chem. Res.* **1982**, *15*, 340−8.

(14) For rollover cycloplatination of the other ligands, see: (a) Minghetti, G.; Stoccoro, S.; Cinellu, M. A.; Soro, B.; Zucca, A. *Organometallics* **2003**, *22*, 4770−4777. (b) Maidich, L.; Zuri, G.; Stoccoro, S.; Cinellu, M. A.; Masia, M.; Zucca, A. *Organometallics* **2013**, *32*, 438−448. (c) Zucca, A.; Cordeschi, D.; Maidich, L.; Pilo, M. I.; Masolo, E.; Stoccoro, S.; Cinellu, M. A.; Galli, S. *Inorg. Chem.* **2013**, *52*, 7717−7731. (d) Zucca, A.; Maidich, L.; Canu, L.; Petretto, G. L.; Stoccoro, S.; Cinellu, M. A.; Clarkson, G. J.; Rourke, J. P. *Chem.−Eur. J.* **2014**, *20*, 5501−5510. (e) Maidich, L.; Dettori, G.; Stoccoro, S.; Cinellu, M. A.; Rourke, J. P.; Zucca, A. *Organometallics* **2015**, *34*, 817−828. For a general review on rollover cyclometalation, see: (f) Butschke, B.; Schwarz, H. *Chem. Sci.* **2012**, *3*, 308−326.

(15) (a) Ravindranathan, D.; Vezzu, D. A. K.; Bartolotti, L.; Boyle, P. D.; Huo, S. *Inorg. Chem.* **2010**, *49*, 8922−8928. (b) Vezzu, D. A. K.; Ravindranathan, D.; Garner, A. W.; Bartolotti, L.; Smith, M. E.; Boyle, P. D.; Huo, S. *Inorg. Chem.* **2011**, *50*, 8261−8273. (c) Harris, C. F.; Vezzu, D. A. K.; Bartolotti, L.; Boyle, P. D.; Huo, S. *Inorg. Chem.* **2013**, *52*, 11711−11722.

(16) For discussion on aromaticity of five-membered cyclopalladated rings, see: Crispini, A.; Ghedini, M. *J. Chem. Soc., Dalton Trans.* **1996**, 75−80.

(17) Fang, Y.-Q.; Hanan, G. S. *Synlett* **2003**, 852−854.

(18) Frisch, M. J.; Trucks, G. W.; Schlegel, H. B.; Scuseria, G. E.; Robb, M. A.; Cheeseman, J. R.; Scalmani, G.; Barone, V.; Mennucci, B.; Petersson, G. A.; Nakatsuji, H.; Caricato, M.; Li, X.; Hratchian, H. P.; Izmaylov, A. F.; Bloino, J.; Zheng, G.; Sonnenberg, J. L.; Hada, M.; Ehara, M.; Toyota, K.; Fukuda, R.; Hasegawa, J.; Ishida, M.; Nakajima, T.; Honda, Y.; Kitao, O.; Nakai, H.; Vreven, T.; Montgomery, J. A., Jr.; Peralta, J. E.; Ogliaro, F.; Bearpark, M.; Heyd, J. J.; Brothers, E.; Kudin, K. N.; Staroverov, V. N.; Kobayashi, R.; Normand, J.; Raghavachari, K.; Rendell, A.; Burant, J. C.; Iyengar, S. S.; Tomasi, J.; Cossi, M.; Rega, N.; Millam, M. J.; Klene, M.; Knox, J. E.; Cross, J. B.; Bakken, V.; Adamo, C.; Jaramillo, J.; Gomperts, R.; Stratmann, R. E.; Yazyev, O.; Austin, A. J.; Cammi, R.; Pomelli, C.; Ochterski, J. W.; Martin, R. L.; Morokuma, K.; Zakrzewski, V. G.; Voth, G. A.; Salvador, P.; Dannenberg, J. J.; Dapprich, S.; Daniels, A. D.; Farkas, Ö.; Foresman, J. B.; Ortiz, J. V.; Cioslowski, J.; Fox, D. J. *Gaussian 09*, Revision D.01; Gaussian, Inc.: Wallingford, CT, 2009.

(19) Zhao, Y.; Truhlar, D. G. *Theor. Chem. Acc.* **2008**, *120*, 215−241.

(20) Weigend, F.; Ahlrichs, R. *Phys. Chem. Chem. Phys.* **2005**, *7*, 3297−3305.

(21) Dunning, T. H. *J. Chem. Phys.* **1989**, *90*, 1007−1023.

(22) Tomasi, J.; Mennucci, B.; Cammi, R. *Chem. Rev.* **2005**, *105*, 2999−3093.

DOI: 10.1021/acs.organomet.5b00326
Organometallics XXXX, XXX, XXX−XXX